This article has been accepted for inclusion in a future issue of this journal. Content is final as presented, with the exception of pagination.

Photonic Crystal as a Section of Modulation and Interaction With a Virtual Cathode in Two-Section Vircator

Artem A. Badarin, Andrey V. Andreev, and Semen A. Kurkin

***Abstract*—We propose and investigate the new scheme of a two-section vircator with a photonic crystal (PC) as a section of modulation and interaction with a virtual cathode (VC). The model demonstrates the high stability of the generation frequency for such type of devices and the electronic efficiency of the order of 12.8%. We achieve this result by implementing a feedback mechanism that stabilizes the frequency and increases the generation efficiency. We show that the primary generation mechanism in the proposed scheme is based on the preliminary modulation of a beam passing through the PC and forming a VC. The model is also characterized by distributed feedback inside the PC, which ensures the effective interaction of a VC with the field in the PC due to spatial synchronism. This regime arises when the beam current lies between the critical currents for each of the sections. The advantages of the proposed scheme include operating in a wide range of values of the beam energy and current, relative design simplicity, and scalability.**

***Index Terms*—Critical current, high-power microwaves, microwave generator, photonic crystal (PC), vircator, virtual cathode (VC).**

I. Introduction

INVESTIGATION and development of devices based on intense electron beams interacting with electromagnetic fields in a vacuum or gas-filled space of electrodynamic systems remain one of the most important and urgent problems of plasma physics and high-power electronics. Such devices are applied in various areas, including the problems of accelerating electron and ion beams, plasma physics, technological processes, problems of long-range radar, and remote sensing of the atmosphere [1]. Generators of ultrahigh-power radiation of the centimeter and millimeter range based on a virtual cathode (VC) (vircators, reditrons, virtodes, and others) have a special place here [2]–[13]. This is conditioned by their unique properties: high output power, simplicity of design, low requirements for beam quality, and the ability to operate without an external magnetic field. At the same time, vircators have significant disadvantages. First of all, this is low stability of the generation frequency and low efficiency, which, as a rule, does not exceed 3%. Note that both problems are interrelated and are primarily due to weak positive feedback in the system and the absence of internal mechanisms for stabilization of generation frequency [1], [14].

The introduction of additional positive feedback in the devices with VC has a positive effect on output power and efficiency and stabilizes electromagnetic radiation frequency. The example of the vircator system with additional feedback is a virtode studied in the works [8], [15]–[18]. In virtode, the injected electron beam passes through two connected sections. The first section plays the role of a modulator, and the second is an interaction chamber designed for the formation of a VC and subsequent energy exchange. Additional electromagnetic feedback is realized due to an electromagnetic wave penetrating through the feedback window from the second section to the first, making it possible to increase the efficiency and stability of the virtode radiation frequency.

Another promising idea is the use of photonic crystals (PC) in VC-based devices [19]. PCs have already demonstrated their effectiveness in vircator schemes [7], [20]. For example, the work [7] has shown that a PC located in a drift tube of the one-section vircator can significantly increase the system's efficiency, compared to a traditional cylindrical waveguide due to several factors: high impedance of the interaction between PC and transmitted electron beam, the feedback in PC, and more efficient accumulation and extraction of electromagnetic energy.

In this work, we propose and investigate the new two-section scheme of VC-based generator, in which PC is used both as a modulation section and as a space for interaction of VC with electromagnetic fields. This approach makes it possible to use the advantages of the virtode scheme (namely, modulation of the beam, forming the VC) and the unique properties of a PC, which implements the distributed electromagnetic feedback with the VC.

Moreover, studying the processes of interaction of relativistic electron beams with high-power electromagnetic fields in vircator systems is also of apparent fundamental importance.

Manuscript received September 4, 2020; revised October 13, 2020 and November 1, 2020; accepted November 4, 2020. This work was supported by the Russian Foundation for Basic Research under Grant 18-32-20135. The review of this article was arranged by Editor J. Feng. *(Corresponding author: Semen A. Kurkin.)*

The authors are with the Centre for Technologies in Robotics and Mechatronics Components, Innopolis University, Innopolis 420500, Russia (e-mail: kurkinsa@gmail.com).

Color versions of one or more figures in this article are available at https://doi.org/10.1109/TED.2020.3037278.

Digital Object Identifier 10.1109/TED.2020.3037278

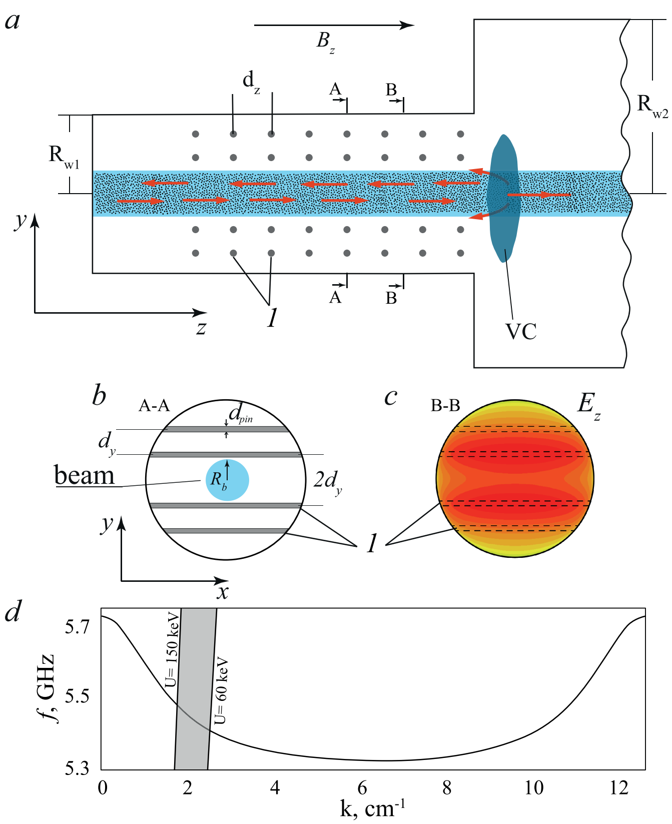

Fig. 1. Scheme of two-section vircator with PC and a beam in squeezed state inside the PC. (a) Schematic representation in the *zy* plane. The blue areas correspond to the electron beam; *1* is the PC; $d_y = 4.75$ mm and $d_z = 5$ mm are the distances between the pins of the PC in the transverse and longitudinal directions, respectively, relative to the direction of propagation of the electron beam. (b) Schematic in the *xy* plane. $d_{\mathrm{pin}} = 1$ mm is the diameter of the conductive pins, and R_b is the radius of the beam. (c) Distribution of the longitudinal component of the excited mode's electric field in the PC. (d) Dispersion characteristic of the excited mode in the PC (cold calculations). Two bold black lines in (d) correspond to the characteristics of undisturbed drifting electron beams with energies 150 and 60 keV, which are defined as $f(k) = v_{bk}/2\pi$, where v_b is the beam drift velocity.

It will help to advance in understanding the complex nonlinear processes occurring in systems with VC. These processes are usually caused by the development of beam instabilities leading, in particular, to the formation of nonstationary space–time electronic structures and the excitation of electromagnetic radiation with a complex spectral composition [21]–[30].

A. Design of the Proposed Scheme

The scheme of the developed two-section vircator generator with PC is presented in Fig. 1. The sections have the form of a cylindrical waveguide. The radius of the first section is $R_{w1} = 15$ mm, of the second — $R_{w2} = 30$ mm. The PC is in the first section. All elements of the system are perfect electric conductors. There is no central conductor in the PC to reduce beam subsidence. The elements of the PC are grounded. A monovelocity cylindrical electron beam with a radius of $R_b = 4$ mm is injected into the system. An external leading magnetic field $B = 1$ T is applied to the system, which passes the beam through the PC and then leads it to the second section's walls. We have chosen the geometrical parameters of the system for operation in the centimeter wavelength range, as the most typical for vircator systems. The magnitude of the magnetic field is chosen such that it limits the deposition of the beam on the PC at all investigated values of the energy and current of the beam. At the right end of the second section, the absorbing boundary condition is used. In this work, we varied beam current in the range 100–700 A and beam energy—in the range 60–150 keV. When the beam with a supercritical current is injected, a VC is formed in the second section, and it reflects part of the beam back into the section with PC.

It is well known that the preliminary modulation of the electron beam in VC-based devices (e.g., in a virtode [8], [15], [17], [18], [31]) increases power, efficiency, and frequency stability of output electromagnetic radiation. We utilize this effect, applying a PC as an additional section for the modulation of a passing electron beam. Besides, the properties of the PC make it possible to create distributed volume feedback, which has a positive effect on the efficiency of VC oscillators.

The main idea of using PC in the proposed scheme is that the injected electron beam excites the fundamental PC mode (Fig. 1(c) shows the configuration of the excited mode); the mode modulates the passing electron beam, which, reaching the second section, forms a VC. The VC starts generating at the frequency of the excited mode and reflects part of the beam back into the PC. Cumulatively, this leads to the appearance of positive feedback between the electromagnetic field and the VC. The frequency of the output radiation is determined primarily by the geometric parameters of the PC. In the operating regime of the system, the beam current must be higher than the critical current for the second section and lower than the critical current for the first section. One of the essential properties of a PC for the functioning of the proposed scheme is the flatness of its dispersion characteristics. This feature makes it possible to ensure efficient interaction of the beam with the PC field in a wide energy range [see Fig. 1(d)], which is especially important for systems with VC, characterized by a large spread in velocities.

Thus, the proposed scheme's key features are the two-section geometry with the PC in the first section, combined with a VC formation in the second section.

We used the 3-D particle-in-cell (PIC) electromagnetic code to study complex nonstationary processes of electron-wave interaction in the proposed high-power microwave device [32], [33]. PIC code is widely used as an effective tool for the simulation of vacuum and plasma systems [33]–[39].

II. Output Characteristics of the Proposed Generator

We have analyzed the output characteristics of the proposed scheme. The dependence of the electronic efficiency in the plane of the control parameters "beam current I is the energy of the electron beam U" is shown in Fig. 2(a). One can see that the generator's electronic efficiency tends to grow with increasing energy and current of the injected beam when they lie in the region between the dependencies of the

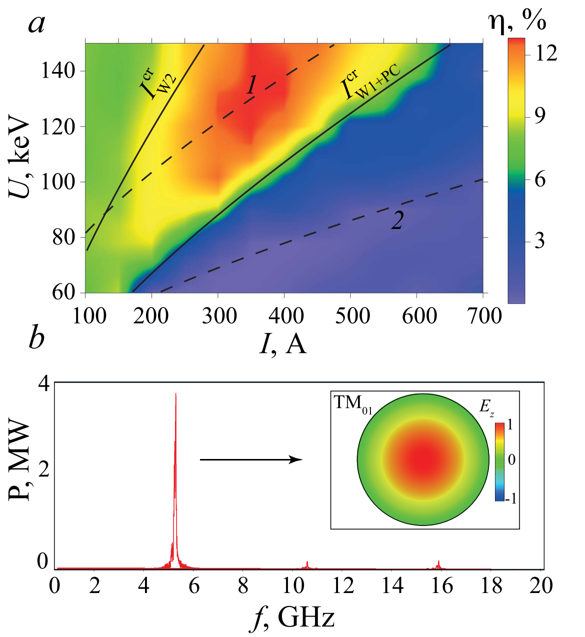

Fig. 2. (a) Electronic efficiency of the proposed generator versus beam energy U and current I. The solid curves show the dependencies of the critical currents I^{cr}_{W1+PC} and I^{cr}_{W2} for the first and the second sections of the vircator, respectively; the dashed curves *1* and *2* determine the values of U and I for which the ratio of the length of the space-charge fast wave to the longitudinal period of the PC $((\lambda/d_z)$, where $\lambda = (2\pi v/\omega + \omega_p)$, v is the beam velocity, and ω and ω_p are the generation frequency and plasma frequency that are 4 and 3, respectively. (b) Frequency spectrum of output electromagnetic radiation at the parameters U and I lying in the region of the maximum electronic efficiency. Inset: working mode (TM_{01}) configuration, which is excited in the output waveguide.

critical currents for the first and the second sections of the vircator (between the curves I^{cr}_{W1+PC} and I^{cr}_{W2}, respectively). The maximum electronic efficiency of 12.8% is achieved at $U = 140$ keV and $I = 385$ A, which is a high value for VC-based generators.

Fig. 2(b) shows the frequency spectrum of output electromagnetic radiation at the control parameters lying in the region of the maximum efficiency. The spectrum has one well-pronounced component at the frequency of 5.3 GHz, which corresponds to the excited electromagnetic mode shown in Fig. 1(c). This indicates the effective interaction of the beam with only one PC mode.

We emphasize that the critical current of an electron beam is one of the most important parameters of the systems with a VC [1], [40]–[42]. When the beam current overcomes the critical value, a VC is formed in the system. For the investigated two-section vircator with the PC, the critical currents' values for two sections (the critical current for the first section with the PC—I^{cr}_{W1+PC} and the critical current for the second section—I^{cr}_{W2}) determine the dynamics of the instabilities development leading to both the formation of VC and the development of a squeezed state in the beam. Fig. 2(a) shows the numerically obtained dependencies of the critical currents I^{cr}_{W1+PC} and I^{cr}_{W2} versus beam energy overimposed on the efficiency distribution. One can see that the efficiency optimum is located between these curves when the beam current exceeds the critical one for the second section and is less than the critical current for the first section ($I^{cr}_{W2} < I < I^{cr}_{W1+PC}$).

III. Dynamics of the System

First of all, we consider in general terms the processes developing in the proposed generator. This scheme is characterized by complex nonlinear dynamics determined by the development of several nonlinear processes. Primarily, it is the process of interaction of intense electron beam with the eigenmodes of the PC, as well as the processes of instabilities development leading to the formation of VC and squeezed state. The squeezed state of the electron beam was first investigated in work [43], where its formation was shown to occur in the systems with a jump in drift tube radius along the beam's propagation direction. When the electron beam with a supercritical current propagates in the system with such geometry, VC forms in the section with a larger radius (R_{w2} in the considered scheme), reflecting a part of the electron beam into the section with a smaller radius (R_{w1}) and forming a two-stream state in it. Then, the instability develops, leading to the formation of a squeezed state in the first section [43]. The transition from a two-stream state to a squeezed one has a wave character and occurs toward the direction of beam propagation. Note that an electron beam in a squeezed state is characterized by a large spread in velocities and a high space-charge density.

A. Basic Generation Regime

To reveal the physical processes occurring in the proposed system and explain the main trends in the presented in Fig. 2(a) dependence of the electronic efficiency, it is necessary to analyze in detail the dynamics of electron beam both in time and when changing the control parameters. Fig. 3(a) shows the evolution of phase portraits in the coordinates (z, v_z) at the control parameters lying in the maximum efficiency region ($U = 140$ keV, $I = 385$ A). The passing electron beam excites an electromagnetic field in the PC, which in turn modulates the electron beam. When the modulated electron beam reaches the second section, VC is formed here, and it reflects part of the beam to the first section with the PC (see Fig. 3(a), $t = 7$ ns). VC oscillates at the modulation frequency of the beam. Then, the instability leading to the formation of a squeezed state develops, and it is accompanied by the VC's motion to the injection plane. In this regime, the beam squeezed state is just a stage in the transient process. One can see clearly that already at time $t = 10.5$ ns, the VC is better developed and located inside the PC in the first section. Simultaneously, the accumulation of energy in the PC field and the buildup of VC oscillations continue. Strong positive feedback arises between the field of the PC and the electron beam with the VC: intense oscillations of the VC pump energy into the PC field, which enhances the modulation of the passed beam and amplifies the VC oscillations.

After the transition process, the stable dynamic regime is established in the system, which is characterized by the presence of several intense VCs inside the PC and vortex electron structures due to the strong turbulence of counter-propagating

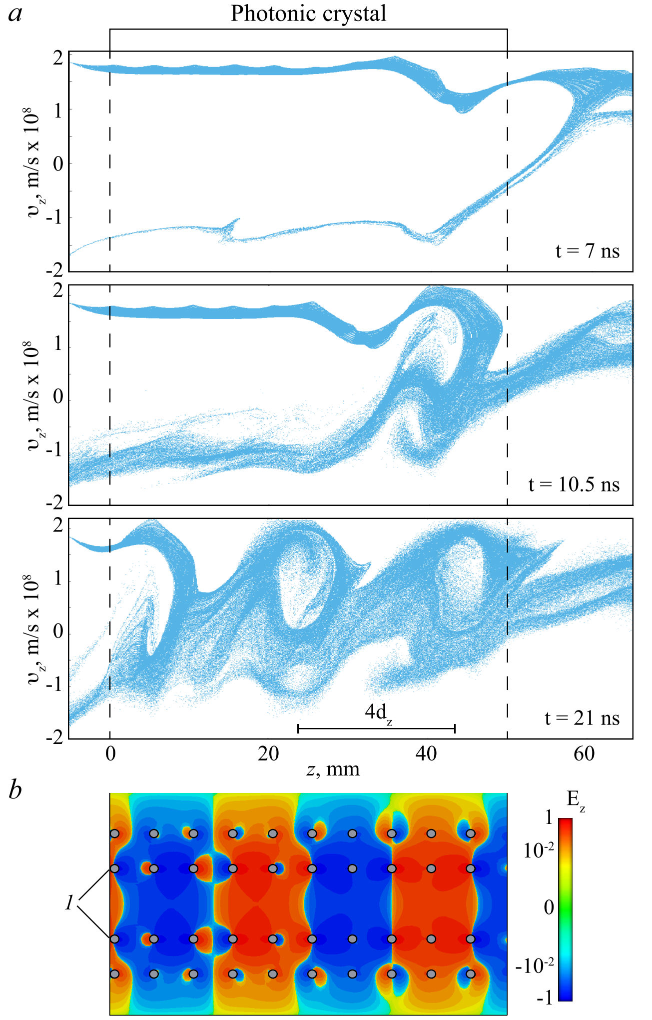

Fig. 3. (a) Series of the phase portraits of the electron beam in the system in the coordinates (z, υ_z) (where z is the longitudinal coordinate of electrons and υ_z is the longitudinal velocity of electrons) for the time moments indicated in the figure. (b) Configuration of the longitudinal component of the electric field strength of the excited mode in the PC. The electron beam energy is $U = 140$ keV, and the current is $I = 385$ A; *1* is the PC.

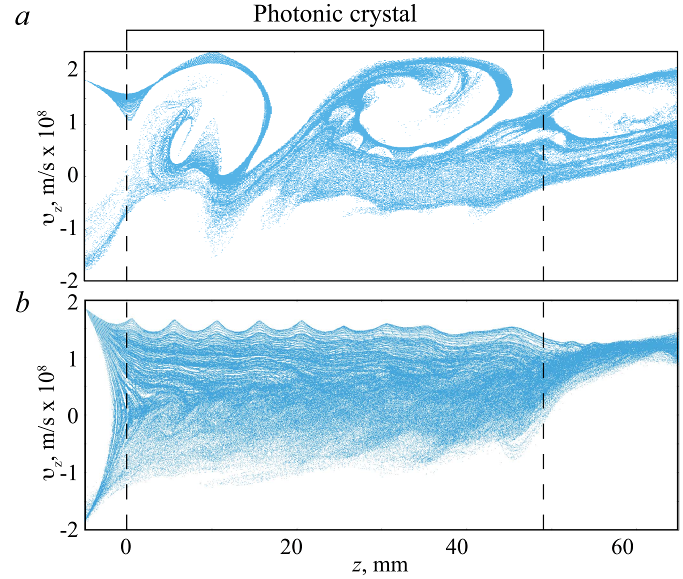

Fig. 4. Phase portraits of the electron beam in the system in the coordinates (z, υ_z) for (a) subcritical regime (beam energy $U = 140$ keV and current $I = 100$ A). (b) Case of generation breakdown ($U = 140$ keV and $I = 700$ A).

beams (see Fig. 3(a), $t = 21$ ns). Such configuration with several VCs results from the interaction of the electron beam with the electric field in the PC (Fig. 3(b) shows the distribution of the electric field longitudinal component E_z in the PC region). One can see that E_z field of the exciting PC mode is in good agreement with the spatial beam structure, and the PC field interacts effectively with the fast space-charge wave. Fig. 3(a) ($t = 21$ ns) shows the length of the fast space-charge wave ($4d_z$), which determines the scale of the emerging space–time electron structures. In particular, the characteristic distance between the adjacent VCs equals four longitudinal periods d_z of the PC.

When an integer number of longitudinal periods of the PC corresponds to the length of the fast space-charge wave, the regime is the most efficient for the energy exchange. Fig. 2(a) shows the dotted curves *1* and *2* defining the beam parameters at which the ratio of the length of the space-charge fast wave to the longitudinal period of the PC is 4 and 3, respectively. One can see that curve *1* is in good agreement with the maximum of efficiency. Curve *2* is in the region corresponding to generation breakdown.

B. Subcritical Regime and Generation Breakdown

In the subcritical regime, when the beam current is less than the critical value for the first and second sections ($I < I^{cr}_{W2} < I^{cr}_{W1+PC}$), reflections of electrons occur at the boundary between the sections, though the value of the injected current is less than critical. This occurs because the electron beam passing through the PC excites the electromagnetic field in the PC, energy is accumulated in this structure, and, as a consequence, the beam modulation is enhanced. When the beam's modulation becomes intense enough that the instant current of a part of the beam exceeds the critical one for the second section, reflections appear at the boundary between the sections, and a VC forms. A two-stream beam state appears in the PC, but the VC movement to the injection plane occurs slowly, since a part of reflected electrons is low. Simultaneously, the accumulation of energy in the PC continues—the beam modulation depth increases, which, combined with the two-stream state, leads to the turbulence of the electron beam and the formation of the vortex structures [they are visible in Fig. 4(a)]. Note that only a small part of electrons return to the injection plane in this regime, and the effect of beam overmodulation plays a significant role, rather than the formation of a VC in the classic sense. Thus, the generation mechanism in the subcritical regime corresponds to that described in work [20] and is based on the PC mode excitation. Electronic efficiency is relatively high in this regime and reaches 9% [see Fig. 2(a)].

In the case when the beam current is higher than the critical values for both sections ($I > I^{cr}_{W1+PC} > I^{cr}_{W2}$), the dynamics of the electron beam is similar to the case when the beam current exceeds the critical one only for the second section. First, a VC is formed in the second section of the vircator in a premodulated beam passing through the PC, which is associated with a higher critical current value for the first section. Then, the instability develops in the beam accompanied by a rapid motion of the VC to the injection plane and the formation of a state similar to the squeezed state of the beam inside the PC [see Fig. 4(b)]. Finally, the stable regime is established in the system, in which the VC is formed directly upon the PC's entry. This leads to the termination of the beam premodulation and the violation of the feedback loop in the system. The development of the squeezed state in the beam in the PC region degrades the efficiency of the interaction between the electron beam and an electromagnetic field in the PC due to the large spread in electrons velocities. Taken together, this leads to a sharp drop in generation efficiency—generation breakdown, which is seen in Fig. 2(a). This regime is similar to the work described in [7] when the parameters of the considered system are not optimal.

IV. Conclusion

We have proposed and investigated a new model of a two-section vircator with a PC, characterized by high stability of the generation frequency for such type of devices and electronic efficiency of the order of 12.8%. Note that vircator systems are usually characterized by switching the generation frequency, which is associated with the absence of internal stabilization frequency mechanisms [14]. In the proposed scheme, switching of the generation frequency is not observed [see Fig. 2(b)]. This result is achieved due to the feedback mechanism that stabilizes the frequency and increases the generation efficiency. We have shown that the principal generation mechanism in this scheme is based on preliminary modulation of the beam passing through the PC and forming the VC. The distributed feedback is realized in the scheme inside the PC and ensures the effective interaction of the VC with the PC electromagnetic field due to their spatial synchronism. This regime is developed when the beam current lies between the critical currents for each of the sections. When the beam current overcomes both critical values, the VC is formed directly upon entering the PC, which leads to a violation of the optimal generation mechanism due to the termination of preliminary beam modulation and the development of a squeezed state. The advantages of the proposed scheme include operating in a wide range of values of the beam energy and current, relative design simplicity, and scalability. Frequency tuning can be realized by changing the configuration of the PC (distance between pins, number of pins, and so on).

References

[1] J. Benford, J. A. Swegle, and E. Schamiloglu, *High Power Microwaves* (Series in Plasma Physics), 3rd ed. Boca Raton, FL, USA: CRC Press, 2016.

[2] S. Mumtaz, J. S. Lim, B. Ghimire, S. W. Lee, J. J. Choi, and E. H. Choi, "Enhancing the power of high power microwaves by using zone plate and investigations for the position of virtual cathode inside the drift tube," *Phys. Plasmas*, vol. 25, no. 10, Oct. 2018, Art. no. 103113.

[3] V. D. Selemir, A. E. Dubinov, V. V. Voronin, and V. S. Zhdanov, "Key ideas and main milestones of research and development of microwave generators with virtual cathode in RFNC-VNIIEF," *IEEE Trans. Plasma Sci.*, vol. 48, no. 6, pp. 1860–1867, Jun. 2020.

[4] R. Cheng *et al.*, "An efficient all cavity axial extraction relativistic magnetron with virtual cathode," *IEEE Trans. Electron Devices*, vol. 67, no. 5, pp. 2165–2169, May 2020.

[5] S. Mumtaz *et al.*, "Enhancement in the power of microwaves by the interference with a cone-shaped reflector in an axial vircator," *Results Phys.*, vol. 15, Dec. 2019, Art. no. 102611.

[6] A. E. Dubinov and V. P. Tarakanov, "Simulation of a magnetically isolated vircator with an under-limit electron beam," *Plasma Phys. Rep.*, vol. 46, no. 5, pp. 570–573, May 2020.

[7] N. Frolov, S. Kurkin, A. Koronovskii, A. Hramov, and A. Rak, "High-efficiency virtual cathode oscillator with photonic crystal," *Appl. Phys. Lett.*, vol. 113, Jul. 2018, Art. no. 023503.

[8] S. A. Kurkin, N. S. Frolov, A. O. Rak, A. A. Koronovskii, A. A. Kurayev, and A. E. Hramov, "High-power microwave amplifier based on overcritical relativistic electron beam without external magnetic field," *Appl. Phys. Lett.*, vol. 106, Apr. 2015, Art. no. 153503.

[9] Y. A. Kalinin, A. V. Starodubov, and A. S. Fokin, "Hybrid vircator microwave oscillator with a nonlaminar electron beam and an electrodynamic section," *Plasma Phys. Rep.*, vol. 45, no. 8, pp. 770–776, Aug. 2019.

[10] R. Verma *et al.*, "Characterization of high power microwave radiation by an axially extracted vircator," *IEEE Trans. Electron Devices*, vol. 61, no. 1, pp. 141–146, Jan. 2014.

[11] J. G. Leopold, Y. P. Bliokh, M. Siman-Tov, and Y. E. Krasik, "Generation of high-current pulses by a magnetized squeezed electron beam," *Phys. Plasmas*, vol. 26, no. 9, Sep. 2019, Art. no. 093107.

[12] M. Mahto and P. K. Jain, "Study of virtual cathodes formation during beam-wave interaction in the reltron oscillator," *Phys. Plasmas*, vol. 24, no. 9, Sep. 2017, Art. no. 093107.

[13] M. I. Fuks, S. Prasad, and E. Schamiloglu, "Efficient magnetron with a virtual cathode," *IEEE Trans. Plasma Sci.*, vol. 44, no. 8, pp. 1298–1302, Aug. 2016.

[14] W. Jiang, "Time–frequency analysis of virtual-cathode oscillator," *IEEE Trans. Plasma Sci.*, vol. 38, no. 6, pp. 1325–1328, Jun. 2010.

[15] N. P. Gadetskii, I. I. Magda, S. I. Naisteter, Y. V. Prokopenko, and V. I. Chumakov, "The virtode: A generator using supercritical REB current with controlled feedback," *Plasma Phys. Rep.*, vol. 19, no. 4, pp. 273–276, 1993.

[16] A. S. Shlapakovski, T. Queller, Y. P. Bliokh, and Y. E. Krasik, "Investigations of a double-gap vircator at submicrosecond pulse durations," *IEEE Trans. Plasma Sci.*, vol. 40, no. 6, pp. 1607–1617, Jun. 2012.

[17] V. D. Selemir, A. E. Dubinov, E. E. Dubinov, I. V. Konovalov, and A. V. Tikhonov, "A hybrid microwave generator based on a vircator-TWT (Virtode) system," *Tech. Phys. Lett.*, vol. 27, no. 7, pp. 583–585, Jul. 2001.

[18] A. A. Badarin, S. A. Kurkin, N. S. Frolov, A. O. Pak, and A. E. Khramov, "Analysis and optimization of the characteristics of superpower virtode generation," *Tech. Phys.*, vol. 64, no. 3, pp. 399–403, Mar. 2019.

[19] V. G. Baryshevsky and A. A. Gurinovich, "Hybrid systems with virtual cathode for high power microwaves generation," 2009, *arXiv:0903.0300*. [Online]. Available: http://arxiv.org/abs/0903.0300

[20] A. A. Badarin, S. A. Kurkin, N. S. Frolov, A. A. Koronovskii, A. E. Hramov, and A. O. Rak, "Higher-order modes excitation in generator with photonic crystal," *Results Phys.*, vol. 15, Dec. 2019, Art. no. 102758.

[21] S. Mumtaz, L. N. Nguyen, H. Uhm, P. Lamichhane, S. W. Lee, and E. H. Choi, "A novel approach to form second virtual cathode by installing a floating zone plate inside the drift tube," *Results Phys.*, vol. 17, Jun. 2020, Art. no. 103052.

[22] A. E. Hramov, A. A. Koronovskiy, S. A. Kurkin, and I. S. Rempen, "Chaotic oscillations in electron beam with virtual cathode in external magnetic field," *Int. J. Electron.*, vol. 98, no. 11, pp. 1549–1564, Nov. 2011.

[23] A. A. Badarin, S. A. Kurkin, A. A. Koronovskii, A. E. Hramov, and A. O. Rak, "Processes of virtual cathodes interaction in multibeam system," *Phys. Plasmas*, vol. 25, no. 8, Aug. 2018, Art. no. 083110.

[24] A. A. Badarin, S. A. Kurkin, A. A. Koronovskii, A. O. Rak, and A. E. Hramov, "Simulation of the development and interaction of instabilities in a relativistic electron beam under variation of the beam wall thickness," *Plasma Phys. Rep.*, vol. 43, no. 3, pp. 346–353, Mar. 2017.

[25] S. A. Kurkin, A. A. Badarin, A. A. Koronovskii, and A. E. Hramov, "Higher harmonics generation in relativistic electron beam with virtual cathode," *Phys. Plasmas*, vol. 21, no. 9, Sep. 2014, Art. no. 093105.

[26] S. A. Kurkin, A. A. Koronovskii, and A. E. Hramov, "Output microwave radiation power of low-voltage vircator with external inhomogeneous magnetic field," *Tech. Phys. Lett.*, vol. 37, no. 4, pp. 356–359, Apr. 2011.

[27] S. A. Kurkin, A. A. Badarin, A. A. Koronovskii, and A. E. Hramov, "The development and interaction of instabilities in intense relativistic electron beams," *Phys. Plasmas*, vol. 22, no. 12, Dec. 2015, Art. no. 122110.

[28] N. S. Frolov, S. A. Kurkin, A. A. Koronovskii, and A. E. Hramov, "Nonlinear dynamics and bifurcation mechanisms in intense electron beam with virtual cathode," *Phys. Lett. A*, vol. 381, no. 28, pp. 2250–2255, Jul. 2017.

[29] A. E. Dubinov, A. G. Petrik, S. A. Kurkin, N. S. Frolov, A. A. Koronovskii, and A. E. Hramov, "Virpertron: A novel approach for a virtual cathode oscillator design," *Phys. Plasmas*, vol. 24, no. 7, Jul. 2017, Art. no. 073102.

[30] A. E. Dubinov, A. G. Petrik, S. A. Kurkin, N. S. Frolov, A. A. Koronovskii, and A. E. Hramov, "Beam-plasma instability in charged plasma in the absence of ions," *Phys. Plasmas*, vol. 23, no. 4, Apr. 2016, Art. no. 042105.

[31] V. Y. Muchkaev and V. A. Tsarev, "Hybrid high-power multiple-beam generator with double-gap coupling resonator system," *IEEE Trans. Electron Devices*, vol. 67, no. 7, pp. 2900–2904, Jul. 2020.

[32] C. K. Birdsall and A. B. Langdon, *Plasma Physics Via Computer Simulation*. Abingdon, U.K.: Taylor & Francis, 2005.

[33] S. A. Kurkin, A. A. Badarin, A. A. Koronovskii, N. S. Frolov, and A. E. Hramov, "Modeling instabilities in relativistic electronic beams in the CST particle studio environment," *Math. Models Comput. Simul.*, vol. 10, no. 1, pp. 59–68, Jan. 2018.

[34] A. E. Dubinov and V. P. Tarakanov, "PIC simulation of the dynamics of electrons in a conical vircator," *IEEE Trans. Plasma Sci.*, vol. 44, no. 8, pp. 1391–1395, Aug. 2016.

[35] A. E. Dubinov, S. K. Saikov, and V. P. Tarakanov, "Multivircator as a new highly effective microwave generator with multiple virtual cathodes: Concept and PIC-simulation," *IEEE Trans. Plasma Sci.*, vol. 48, no. 1, pp. 141–145, Jan. 2020.

[36] A. A. Badarin, S. A. Kurkin, A. V. Andreev, A. A. Koronovskii, N. S. Frolov, and A. E. Hramov, "Virtual cathode oscillator with elliptical resonator," in *Proc. 18th Int. Vac. Electron. Conf. (IVEC)*, Apr. 2017, pp. 1–2.

[37] N. S. Frolov *et al.*, "Perspective sub-THz powerful microwave generator 'nanovircator' for T-rays biomedical diagnostics," in *Proc. 3rd Int. Symp. Opt. Biophotonics, 7th Finnish-Russian Photon. Laser Symp., Saratov Fall Meeting (PALS)*, vol. 9917, 2016, Art. no. 991721.

[38] N. S. Phrolov, A. A. Koronovskii, Y. A. Kalinin, S. A. Kurkin, A. V. Starodubov, and A. E. Hramov, "The effect of an external signal on output microwave power of a low-voltage vircator," *Phys. Lett. A*, vol. 378, nos. 32–33, pp. 2423–2428, Jun. 2014.

[39] A. Saxena, A. Roy, K. V. Kanakgiri, S. J. Petkar, F. S. Kazi, and N. M. Singh, "Particle-in-cell modeling of axial and coaxial virtual cathode oscillators," *IEEE Trans. Plasma Sci.*, vol. 44, no. 10, pp. 2399–2405, Oct. 2016.

[40] S. A. Kurkin, A. A. Koronovski, and A. E. Hramov, "Nonlinear dynamics and chaotization of oscillations of a virtual cathode in an annular electron beam in a uniform external magnetic field," *Plasma Phys. Rep.*, vol. 35, no. 8, pp. 628–642, Aug. 2009.

[41] A. E. Hramov, S. A. Kurkin, A. A. Koronovskii, and A. E. Filatova, "Effect of self-magnetic fields on the nonlinear dynamics of relativistic electron beam with virtual cathode," *Phys. Plasmas*, vol. 19, no. 11, Nov. 2012, Art. no. 112101.

[42] S. A. Kurkin, A. E. Hramov, and A. A. Koronovskii, "Microwave radiation power of relativistic electron beam with virtual cathode in the external magnetic field," *Appl. Phys. Lett.*, vol. 103, no. 4, Jul. 2013, Art. no. 043507.

[43] A. M. Ignatov and V. P. Tarakanov, "Squeezed state of high-current electron beam," *Phys. Plasmas*, vol. 1, no. 3, pp. 741–744, Mar. 1994.